CHEMICAL KINETICS
AND CATALYSIS

Structure and Kinetic Properties of a Molten FLiBe Mixture with Tritium

A. Y. Galashev[a,b],*, A. F. Anisimov[a], and A. S. Vorob'ev[a]

[a] *Institute of High-Temperature Electrochemistry, Russian Academy of Sciences,*
Ural Branch, Yekaterinburg, 620137 Russia
[b] *Ural Federal University, Yekaterinburg, 620075 Russia*
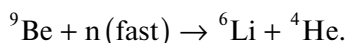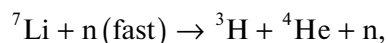***e-mail: galashev@ihte.ru**

Abstract—A study is performed of the self-diffusion of tritium and fluorine atoms, and the change in the structure of molten FLiBe upon raising the temperature of the system from 873 to 1073 K. The interaction between neutrons and both lithium and beryllium in molten-salt reactors (MSR) using FLiBe as a fuel salt results in the formation of large amounts of tritium. Tritium, which easily penetrates metallic structural materials at high temperatures, is a radionuclide hazard. Predictive models for the behavior of tritium in a molten fluoride salt must therefore be developed to solve the problem of MSR safety. The emergence of tritium in the system increases the average energy of interatomic bonds upon raising the temperature and concentration of tritium in the system. A rise in temperature is also accompanied by fluorine atoms creating a closer short-range order in the environment of tritium atoms. This is expressed in the formation of a high first peak of radial distribution function $g_{T-F}(r)$, an increase in the number of probable geometric neighbors, which is shown by Voronoi polyhedra, and fluorine atoms giving priority to fourth-order rotational symmetry in the environment of tritium atoms.

INTRODUCTION

Molten-salt reactors (MSRs) are a promising line in the development of nuclear energy, as they offer high efficiency and safety by using molten salt as a coolant. This allows us to eliminate such shortcomings typical of conventional and boiling water reactors as pressure inside the first circuit and a relatively low boiling point of the coolant. There are concepts of MSRs for both thermal and fast neutrons [1, 2]. An FLiBe melt that is a binary mixture of LiF and BeF_2 salts is an example of what can be used as a coolant in such reactors. FLiBe is chemically stable, low tritium solubility, and low vapor pressure [3]. The viscosity, density, and heat capacity of LiF–BeF_2 and LiF–BeF_2 + UF_4 salt melts at a temperature of 700°C were studied in [4, 5]. Natural lithium consists of 7.42% ^{6}Li and 92.58% ^{7}Li. Tritium (^{3}H) forms in the system due to the absorption of neutrons by its elements. The corresponding reactions are

$$^6Li + n\,(thermal) \rightarrow \,^4He + \,^3H,$$

$$^7Li + n\,(fast) \rightarrow \,^3H + \,^4He + n,$$

$$^9Be + n\,(fast) \rightarrow \,^6Li + \,^4He.$$

The first reaction is key for the production of tritium in thermal MSRs. Additional reactions with ^{7}Li and ^{9}Be, the final products of which are also ^{3}H, are possible in fast MSRs. ^{6}Li is a good neutron absorber, so including it in FLiBe adversely affects the safety of the reactor. The release of tritium upon irradiating samples of FLiBe in a nuclear reactor was studied in [6].

Despite its purification, the salt loaded into the reactor still contained residual ^{6}Li (~0.005%) that captures neutrons and generates tritium (T) nuclides. Tritium is a radioactive isotope of hydrogen with a half-life of 12.32 years. It usually exists in chemical forms TF and HT, but it can also be found as neutral atom T^0 [7]. The solubility of gaseous tritium in molten salt is low. At high temperatures, however, tritium has a relatively high coefficient of diffusion and good solubility in metallic materials. It can therefore migrate from the molten salt in the primary circuit to the second circuit, or to the atmosphere through the heat exchanger tubes. HT can thus diffuse through metal, resulting in hydrogen embrittlement. The TRIDENT model of the evolution and diffusion of tritium was created and tested in [8]. On the other hand, TF appears to be a strong corrosive agent that destroys a structural metal. Tritiated water is an
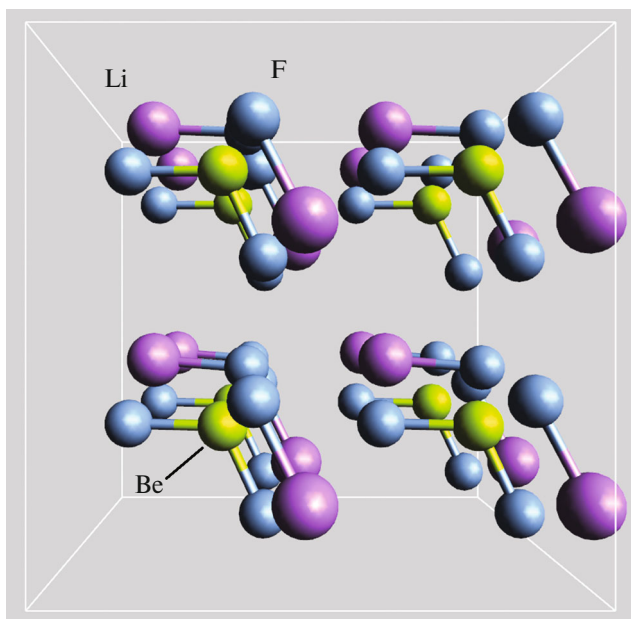
Fig. 1. Initial structure of LiF–BeF$_2$.

extremely dangerous environmental pollutant, so controlling the content of tritium in an MSR is of paramount importance. Graphite is used to adsorb TF and HT. When creating a macromodel of tritium propagation, it is advisable to consider the production, adsorption, corrosion, and penetration of tritium as a generalized characteristic of tritium transport [9].

The aim of this work was to study the behavior of tritium in an FLiBe melt at high temperatures using ab initio molecular dynamics, and to calculate the kinetic, energy, and structural characteristics of the salt melt while giving special attention to establishing the immediate environment around atoms of tritium.

COMPUTER MODEL

We used a cubic cell containing 8 Be, 16 Li, and 32 F atoms to model a LiF–BeF$_2$ melt. The ratio between components LiF and BeF$_2$ was 66 to 34. The densities of the studied systems corresponded to experimental values of FLiBe density at given temperatures [10]. The structure of pure FLiBe (i.e., a system with no impurities) is shown in Fig. 1. Tritium particles were introduced into the system by replacing one or two lithium ions. Modeling was done using the SIESTA software package [11] based on the use of an atom-centered basis set. Inside the radius of containment, strictly limited atomic basic orbitals were products of multiplying a numerical radial function by a spherical harmonic. In this work, we used double-zeta polarized basis set. Our calculation scheme adapted the standard split valence approach to fixed numerical orbitals (i.e., basis orbitals could be reflected by linear combinations of Gaussians). A version of the

SIESTA-4.0-500 program was used. First-principles (ab initio) molecular dynamics modeling was done using a generalized gradient approximation in the form of PBE [12] with a Nose–Hoover thermostat [13] at temperatures of 873, 973, and 1073 K. The time step was 1 fs, and duration of the calculations was ~1200 time steps. The system was relaxed until the change in the total energy of the system was less than 0.001 eV. The density of the three-dimensional grid used to calculate the electron density was set using a cutoff energy of 400 Ry.

For the systems in this work, we calculated

• the average bonds energy in a melt,

$$E_{\text{b}} = -\frac{E_{\text{tot}} - \sum E_i N_i}{N},$$

where E_{tot} is total energy of the system. E_i and N_i are energy and number of i-particles in the melt, respectively (where i = T, Li, F, Be), and $N = \Sigma N_i$ is the number of particles in the melt;

• the bonds energy between the identified compounds of tritium and the rest of the melt,

$$E_{\text{b}}^{\text{TF}_x} = -(E_{\text{tot}} - E_{\text{tot}-\text{TF}_x} - E_{\text{TF}_x}),$$

where $E_{\text{tot}-\text{TF}_x}$ is the energy calculated for the melt without the tritium compound, and E_{TF_x} is the energy calculated for the tritium compound with the melt; and

• the energy of T–F bonding in the identified tritium compounds,

$$E_{\text{b}}^{\text{T–F}} = -(E_{\text{TF}} - E_{1\text{T}} - E_{1\text{F}}),$$

where E_{TF} is the total energy calculated for the atoms constituting T–F bonds, and $E_{1\text{T}}$ and $E_{1\text{F}}$ are the energies calculated for tritium and fluorine in the gas phase.

Coefficient D of the self-diffusion of atoms was determined using the Einstein equation (i.e., the slope of the dependence of the average square of the displacement $\langle \Delta r^2 \rangle$ of the center of mass of homogeneous atoms on time):

$$D = \frac{1}{6} \lim_{t \to \infty} \langle \Delta r^2 \rangle / t,$$

where $\langle \Delta r^2 \rangle$ was calculated according to the expression

$$\langle \Delta r^2 \rangle = \left\langle \frac{1}{N} \sum_{i=0}^{N} \left[r_i(t_0 + dt) - r_i(t_0) \right]^2 \right\rangle$$
$$= \frac{1}{Nn_t} \sum_{i=0}^{N} \sum_{j=0}^{n_t} \left[r_i(t_j + dt) - r_i(t_j) \right]^2,$$

where N is the number of atoms of a certain sort, n_t is the number of intervals for determining $\langle \Delta r^2 \rangle$, t_0 and t_j

Table 1. Average bonding energies among atoms in the system and average Mulliken charges* of atoms at the last step of modeling, depending on the temperature of the melt and the amount of tritium in the system

System	T, K	E_b, eV	Q_{Be}, a.u.	Q_{Li}, a.u.	Q_F, a.u.	Q_T, a.u.
Pure FLiBe	873	4.230	1.087	0.270	−0.407	—
	973	4.229	1.083	0.269	−0.405	—
	1073	4.229	1.095	0.266	−0.407	—
1T	873	4.419	1.084	0.205	−0.415	0.662
	973	4.441	1.086	0.270	−0.417	0.601
	1073	4.479	1.100	0.268	−0.422	0.675
2T	873	4.600	1.071	0.270	−0.425	0.634
	973	4.629	1.066	0.258	−0.421	0.652
	1073	4.655	1.104	0.259	−0.429	0.641

* The atomic unit (a.u.) of a charge is the unit of the elementary charge.

are the initial times, and the angle brackets denote averaging over the chosen equidistant times.

The partial radial distribution function is defined as

$$g_{\alpha\beta} = \frac{dn_{\alpha\beta}(r)}{4\pi r^2 dr \rho_\alpha},$$

where $dn_{\alpha\beta}(r)$ is the number of atoms of type β in layer dr at distance r from an atom of type α. The partial density of the α component is $\rho_\alpha = V/N_\alpha = V/(Nx_\alpha)$, and x_α is the concentration of the α component.

The first coordination number is defined as [14]

$$n_{\alpha\beta} = 4\pi\rho x_\beta \int_0^{r_{min}} r^2 g_{\alpha\beta}(r)dr,$$

where ρ is the numerical density, x_β is the concentration (N_β/N) of component β, and r_{min} is the first minimum of function $g_{\alpha\beta}(r)$.

The detailed structure of the fluorine environment of tritium was studied by means of statistical geometry based on constructing Voronoi polyhedra (VPs) [15, 16]. Neighbors in the form of fluorine atoms were identified through the faces of the polyhedra, each center of which contained a tritium atom. Structural analysis based on constructing the VPs provided more complete three-dimensional information about the structure than the one-dimensional radial distribution function. The topological characteristics traditionally used are the distribution of VPs over the number of faces and distribution of the faces over the number of sides. The former establishes the probability of finding a given number of immediate geometric neighbors around selected atoms. The latter indicates the probability of finding m-membered structural rings when observed from the center of a VP in directions of the location of the immediate geometric neighbors. An important metric characteristic is the angular distribution of the immediate geometric neighbors. When constructing it, we consider angles θ enclosed between pairs of segments connecting the center of a VP with its geometric neighbors (i.e., the vertex of angle θ coincides with the center of the VP, and the sides are perpendicular to the corresponding faces). VPs were built for the configurations obtained at each time step.

All calculations presented here were made on the URAN cluster-type hybrid computer at the Institute of Mathematics and Mechanics, Ural Branch, Russian Academy of Sciences. Different numbers of processors (1 to 5) were used in our systematically extended calculations. With respect to single processor usage, the estimated run time for each of the studied systems was approximately 500 h.

RESULTS AND DISCUSSION

Table 1 presents average bonding energies and Mulliken charges of atoms calculated for a LiF–BeF$_2$ melt, depending on the temperature and composition of the melt. The bonding energies in the pure FLiBe system are constant in the 873 to 1073 K range of temperatures. Substituting one lithium ion for tritium lowers the bonding energy from 4.4 to 5.9%, depending on the temperature of the given system. We can see from Table 1 that the bonding energy grows along with temperature for systems containing tritium. A state with the greatest positive charges for Be is established after the transfer of charges in the given molten salt. Tritium has the next highest positive charge, while lithium has the lowest positive charge. The module of negative charges of F grow negligibly (by a maximum of 5%) when tritium is added to an FLiBe melt.

Figure 2 shows the geometric structures of the pure FLiBe system obtained at temperature of 973 K. In all the pure systems, the first coordination sphere of beryllium includes four fluorine atoms that form a tri-
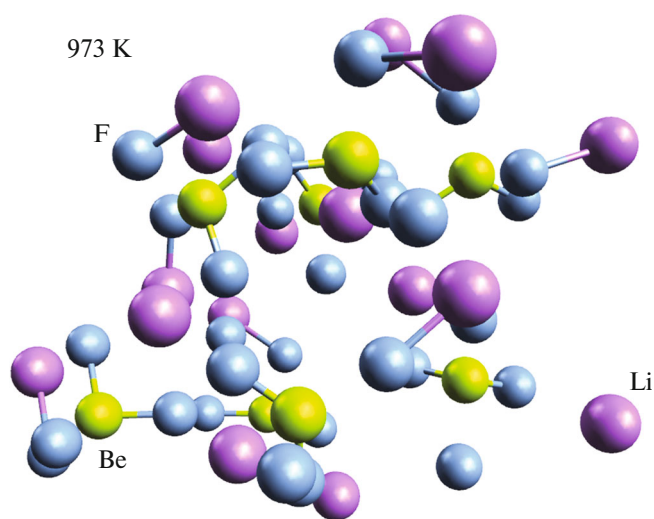
Fig. 2. Geometric structure obtained for our pure FLiBe system at a temperature of 973 K.

angular pyramid (tetrahedron) centered on a beryllium atom. The coordination of beryllium in an FLiBe molten salt containing tritium was studied in [7]. It was shown that two asymmetric tetrahedra, the centers of which contain one beryllium atom each, could be combined with the formation of a common vertex. There were thus 3.5 F atoms for each Be atom.

The first coordination number, determined in terms of partial radial distribution function $g_{Li-F}(r)$, changes from 4.4 to 4.3 upon raising the temperature of the molten salt (LiF–BeF$_2$–T) from 773 to 1073 K [7]. We found that the immediate environment of lithium should contain 3 to 6 F atoms with bond lengths of 1.61 to 2.80 Å and an average length of 2.06 Å. Pos-

sible configurations of the immediate environment of lithium and beryllium are shown in Fig. 3. Replacing a lithium ion with a tritium one does not alter the geometric structures formed by lithium. However, the first coordination sphere of beryllium obtained through calculations can be reduced from four to three fluorine atoms when tritium is introduced into the system. [BeF$_3$]$^-$ ions form due to the formation of the TF compound in the melt, which releases the fluorine ion from the first [BeF$_4$]$^{2-}$ coordination sphere. The average T–F bond lengths change from 1.63 Å for [BeF$_4$]$^{2-}$ to 1.56 Å in the [BeF$_3$]$^-$ complex upon this transition.

Figure 4 shows temporal dependences of the T–F bond lengths at a temperature of 973 K. The upper dependence reflects the change over time in the bond length of a tritium atom with a fluorine atom permanently located near it. The two lower dependences are those of replacing one neighboring fluorine atom with another. One moves away from the tritium atom within 600 fs, while the other starts approaching it at 600 fs. The amplitudes of the fluctuations in bond length for a permanent neighbor are much lower than those of a departing or newly acquired neighbor.

We obtained three temporal dependences of T–F bond lengths for systems containing one tritium atom and six for systems containing two tritium atoms. The behavior of bond lengths over time were different in all cases. However, three average bond lengths can be distinguished on the basis of the obtained data: 1.05, 1.2, and 1.5 Å. These characteristics correspond to the 0.86–1.15, 1–1.3, and 1.3–1.7 Å ranges of bond lengths. The assumptions presented in Fig. 5 about the existence of [TF$_2$]$^-$ and TF compounds are based on these data. The TF compound has a T–F bond length of ~1 Å, while [TF$_2$]$^-$ compounds can be of two types:
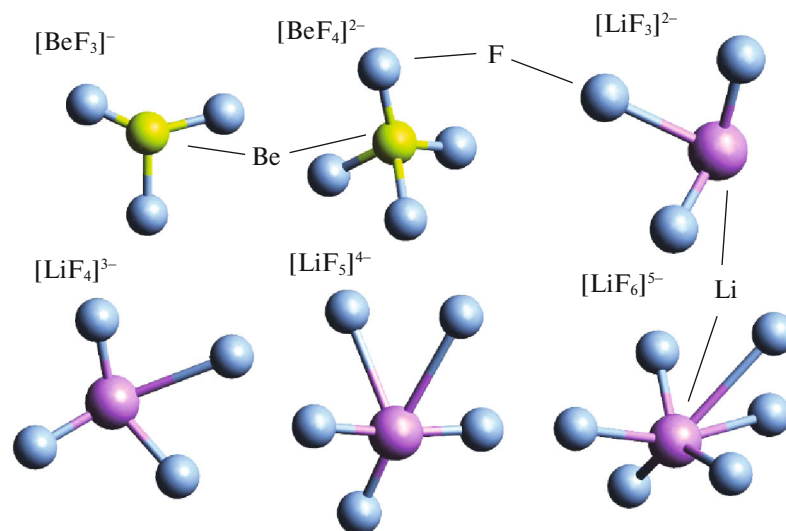

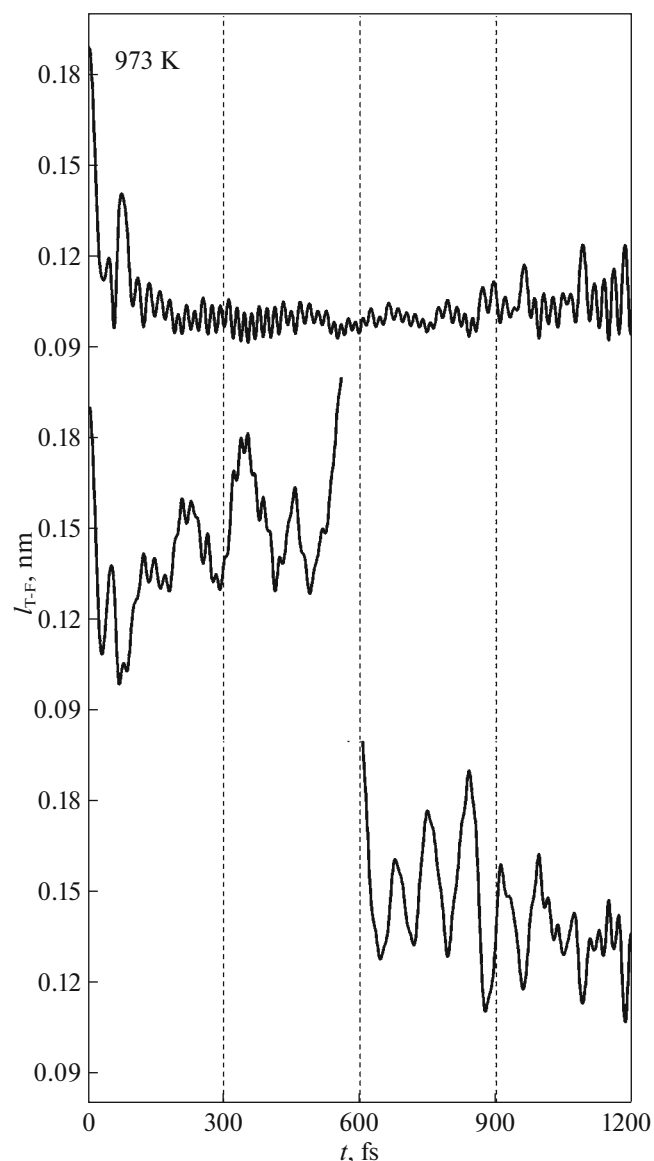**Fig. 3.** Geometric structures of first coordination spheres of beryllium and lithium.

energy of these bonds changes upon moving to a $[TF_2]^-$ compound with different bond lengths: the longer bonds have an energy of ~2.18 eV, and the short ones have ~5.24 eV. A transition from a $[TF_2]^-$ compound with different bond lengths to a TF compound is also possible. When one fluorine atom is held near a tritium atom, a stable TF compound forms with a bonding energy of ~5.37 eV. At the same time, the TF compound has negative energy (−318.9 eV) of bonding with a melt, indicating the release of TF in the form of a gas.

Mean squares of the displacements of tritium and fluorine atoms obtained at temperatures of 873 and 1073 K are shown in Fig. 6. We can see from the figure that dependence $\langle(\Delta r)^2\rangle(t)$ for F atoms was nearly linear at all temperatures (dependence $\langle(\Delta r)^2\rangle(t)$ at $T = 973$ K is not shown in Fig. 6). At the same time, growing dependence $\langle(\Delta r)^2\rangle(t)$ for tritium atoms must be approximated by a linear one in order to determine the corresponding coefficient of self-diffusion. It was shown in [17, 18] that a localized charge slows the dynamics of ions in ionic liquids and molten salts. In other words, the value of the ion charge has a much stronger effect on the coefficient of the self-diffusion of ions than their mass. The calculated coefficients of self-diffusion for the T and F atoms of the FLiBe + 2T system are presented in Table 2. We can see that the coefficients of self-diffusion for the T and F atoms grow along with temperature, and the increase in D for lighter T atoms proceeds much faster. The mobility of ions is in this case determined mainly by their induced charge [19], which is higher for tritium than for fluorine.

In [19], the coefficient of diffusion for tritium in molten salt FLiBe was measured in the 773−973 K range of temperatures. Tritium was in both the atomic form and molecular form T_2 in each experiment. It could bond with T^+ and BeF_4^- ions, or form an HT or other compound. The temperature dependence of the effective coefficient of diffusion took the form

$$D\left[\frac{m^2}{s}\right] = 9.3 \times 10^{-7} \exp\left(-\frac{42154}{RT}\right),$$

where $R = 8.31$ J/(mol K) is molar gas constant.

Fig. 4. Change in T−F bond lengths (l_{T-F}), depending on the duration of the calculations at a temperature of 973 K. The plot are shown for three fluorine atoms.

one with equal T−F bond lengths (~1.2 Å) and another with different T−F bond lengths (~1 and ~1.5 Å). In the $[TF_2]^-$ compound with equal bond lengths, the energy of each bond is ~3.65 eV. The

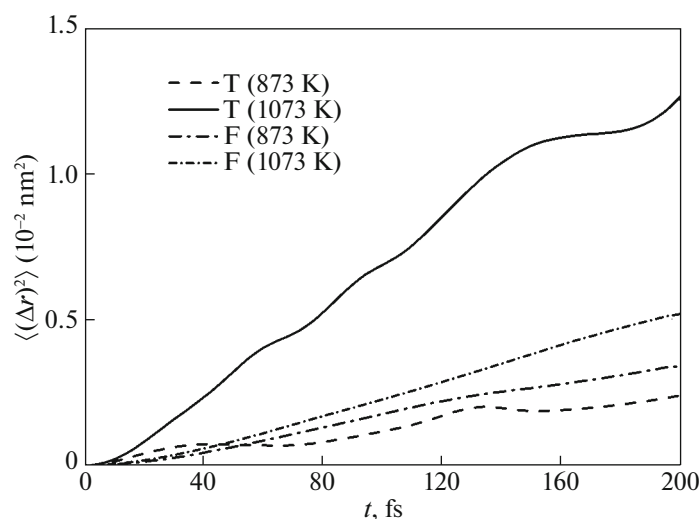**Fig. 5.** Form of the resulting tritium compounds in our system.

Fig. 6. Mean square displacement of atoms in our FLiBe + 2T system at temperatures of 873 and 1073 K.

Experimental values of the effective coefficient of diffusion for tritium [20] are given in Table 2. In contrast to the experimental effective values of D, where tritium diffused through a nickel plate, it was always present in the atomic form in our computer model. The values calculated at high temperatures (973 and 1073 K) are therefore higher than the experimental ones.

The coefficients of self-diffusion for T_2 molecules and the TF compound were calculated via equilibrium molecular dynamics and are presented in Table 2 [20]. The coefficient of self-diffusion calculated for T_2 is on average 2.5 times higher than for TF. This can be explained by correlations in the blending of TF with beryllium fluoride complexes and fluorine in the modeled mixture. The temperature dependence of the D values calculated for T_2 and TF takes the form

$$D[10^{-5}\ cm^2/s] = -44.1694 + 0.0517T\ [K]$$

Table 2. Calculated and experimental coefficients of self-diffusion (in units of 10^{-5} cm^2/s) of atoms T and F, and of T_2 and TF in our FLiBe melt

Atom	873 K	973 K	1073 K
T	1.95	7.60	10.5
T_2 [15]	2.79	5.07	8.25*
T_2 [16]	1.00	6.30	11.35
F	5.8	6.4	8.8
TF [16]	0.95	3.0	6.30

* Extrapolated value obtained from the $D(T)$ curve at lower temperatures.

and

$$D[10^{-5}\ cm^2/s] = -16.7199 + 0.0202T\ [K],$$

respectively.

Partial radial distribution functions $g(r)_{T-F}$ and $g(r)_{T-FLiBe}$ are in many ways similar for systems with one or two T atoms in FLiBe. This is because the tritium atoms are surrounded primarily by fluorine atoms, while the remaining atoms lie at considerable distances from the T atoms and mainly affect the formation of the second coordination sphere. First coordination number n_{T-F} for the systems containing tritium fell slightly as the temperature rose and ranged from 2.13 to 1.86. Function $g(r)_{T-F}$ obtained for the 2T + FLiBe system at temperatures of 873 and 1073 K is shown in Fig. 7. A feature of these functions is that the height of the first peak grows along with temperature, and its location shifts slightly (by 0.005 nm) toward shorter distances. The atypical behavior of the first peak of function $g(r)_{T-F}$ was due to an increase in the chemical bonding of the T and F atoms as the temperature rose. In other words, temperature was the main parameter determining difference $\Delta\mu$ between the chemical potentials of the products and reactants, which is the driving force for the reaction between T and F atoms. This dependence is often presented in the literature as one between thermodynamics and kinetics, and is expressed by the Michaelis–Menten equation [21]

$$\Delta\mu = -RT\ln(J^+/J^-),$$

where R is the universal gas constant, and T is absolute temperature. J^+ and J^- are the flows (rates) of reactions proceeding in the forward and reverse directions,
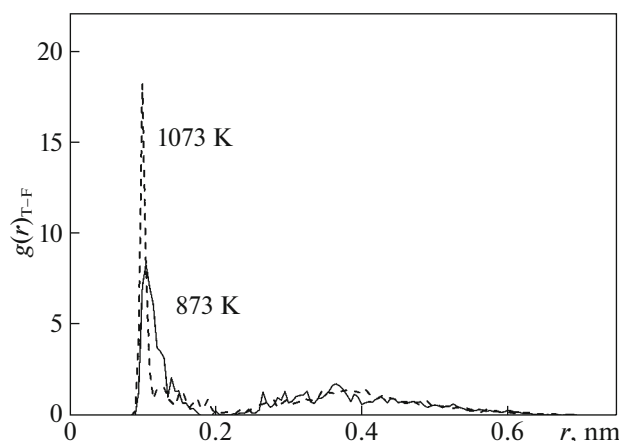
Fig. 7. Partial radial distribution function $g(r)_{T-F}$ for our FLiBe + 2T system at temperatures of 873 and 1073 K.
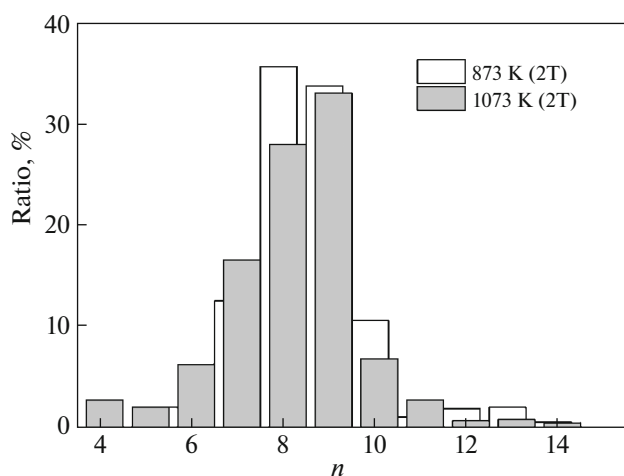

Fig. 8. Distribution of Voronoi polyhedra over the number of faces when constructing VP for tritium atoms surrounded only by fluorine atoms at temperatures of 873 and 1073 K.
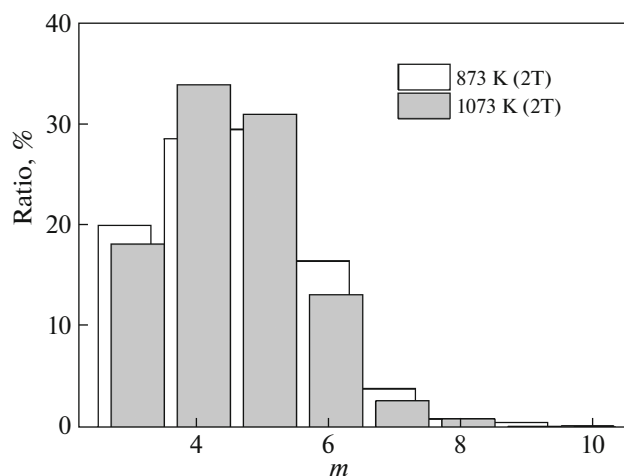

Fig. 9. Distribution of faces of Voronoi polyhedral, according to the number of sides when constructing VP for tritium atoms surrounded only by fluorine atoms at temperatures of 873 and 1073 K.

so the actual rate of the reaction is defined as
$J = J^{+} + J^{-}$.

As reflected by Voronoi polyhedra, the short-range order in the molten salt extends to distances exceeding the outer radius of the first coordination sphere [22]. In other words, the VP faces are created from the neighbors that form both the first and part of the second coordination sphere. It is therefore of interest to study the arrangement of F atoms around tritium atoms. Figure 8 shows the distribution of hybrid VP over the number of faces for the FLiBe + 2T system at temperatures of 873 and 1073 K. The hybrid VP were built around T atoms, and the F atoms served as the environment providing the VP faces. We can see from the figure that the maximum of the n-distribution obtained at 873 K lies at $n = 8$, while the maximum at 1073 K falls on $n = 9$. The creation of more favorable conditions for diffusion (a rise in temperature and a drop in the density of the melt) thus increased the probability of a larger environment of tritium atoms with fluorine atoms.

The distribution of F atoms around T atoms becomes increasingly ordered and predictable as the temperature rises. The joint fraction of the most probable four- and five-sided faces in the distribution of VP faces over the number of sides fell from 58.1 to 65.0% as the temperature of the system rose from 873 to 1073 K (Fig. 9). The proportion of quadrangular faces (34%) also exceeded that of pentagonal faces (31%) at 1073 K. In other words, the fourth-order rotational symmetry inherent in a crystal began to predominate over the fifth-order symmetry typical of disordered systems. At the same time, the fraction of faces with $m \geq 6$ sides fell by 5% as the temperature rose from 873 to 1073 K.

The distribution of angles θ formed by pairs of geometric neighbors F and a tritium atom at the apex is shown in Fig. 10. The θ-distributions shown in the figure were obtained for the FLiBe + 2T system at temperatures of 873 and 1073 K. The maxima of the θ-distributions fall at angles θ of 60° (873 K) and 70° (1073 K). It is at such angles that we most often observe the arrangement of pairs of fluorine atoms from the center of a tritium atom. The expansion of the most probable angle θ correlates with an increase in the number of immediate geometric neighbors of fluorine atoms surrounding the tritium atom. Though it has a jagged outer contour, the domed shape of both distributions indicates the main irregularity in the arrangement of F atoms around the tritium atom [18].

CONCLUSIONS

We modeled LiF−BeF$_2$ molten salt with a constituent component ratio of 66 : 34% and tritium inclusions in the $873 \leq T \leq 1073$ K range of temperatures. It was shown that strong bonds between tritium and
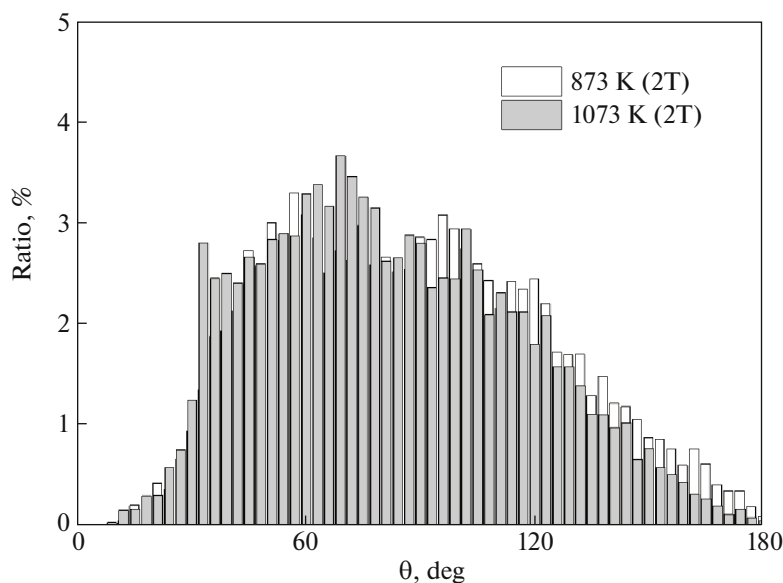
Fig. 10. Angular distribution of the immediate geometric neighbors of fluorine atoms surrounding tritium atoms at temperatures of 873 and 1073 K.

fluorine have yet to be established. Atom T diffuses separately from atoms F, and coefficient D of tritium self-diffusion grows along with temperature faster than that of fluorine. Raising the temperature brings atoms T and F closer and results in more stable short-range ordering of atoms F around atom T. The transfer of charge among atoms in the system was studied. It was found that substituting tritium for lithium in the system raises the average energy of all bonds and can result in a transition from ionic complex $[BeF_4]^{2-}$ to complex $[BeF_3]^-$. Three possible states of tritium in the considered system were established: TF and two compounds $[TF_2]^-$, along with the possibility of transitions between these states.

Understanding the mechanisms of interaction between tritium and an FLiBe melt is important in developing technology for reducing the formation of tritium compounds in an operating MSR and creating conditions for the safe release of accumulated tritium.

FUNDING

CONFLICT OF INTEREST

The authors declare that they have no conflict of interest.

REFERENCES

1. S. H. Yu, Y. F. Liu, P. Yang, et al., Nucl. Sci. Tech. **32** (9) (2021).
   https://doi.org/10.1007/s41365-020-00844-0

2. S. A. Nasser, M. E. Shayan, F. Ghasemzadeh, et al., *Nuclear Power Plants: The Processes from the Cradle to the Grave* (InTech Open, Rijeka, 2021).
   https://doi.org/10.5772/intechopen.90939

3. H. Shishido, N. Yusa, H. Hashizume, et al., Fussion Sci. Technol. **68**, 669 (2017).
   https://doi.org/10.13182/FST14-975

4. A. Redkin, A. Khudorozhkova, E. Il'ina, et al., J. Mol. Liq. **341**, 117215 (2021).
   https://doi.org/10.1016/j.molliq.2021.117215

5. O. Yu. Tkacheva, A. V. Rudenko, A. A. Kataev, P. N. Mushnikov, A. S. Kholkina, and Yu. P. Zaikov, Russ. J. Non-Ferr. Met. **63**, 272 (2022).
   https://doi.org/10.3103/S1067821222030117

6. K. Dolan, G. Zheng, K. Sun, et al., Prog. Nucl. Energy **131**, 103576 (2021).
   https://doi.org/10.1016/j.pnucene.2020.103576

7. H. Wang, B. Yue, L. Yan, et al., J. Mol. Liq. **345**, 117027 (2022).
   https://doi.org/10.1016/j.molliq.2021.117027

8. J. D. Stempien, R. G. Ballinger, and C. W. Forsberg, Nucl. Eng. Des. **310**, 258 (2016).
   https://doi.org/10.1016/j.nucengdes.2016.10.051

9. H. Qin, C. Wang, D. Zhang, et al., Prog. Nucl. Energy **117**, 103064 (2019).
   https://doi.org/10.1016/j.pnucene.2019.103064

10. S. Cantor, W. T. Ward, and C. T. Moynihan, J. Chem. Phys. **50**, 2874 (1969).

11. J. M. Soler, E. Artacho, J. D. Gale, et al., J. Phys.: Condens. Matter **14**, 2745 (2002).
    https://doi.org/10.1088/0953-8984/14/11/302

12. J. P. Perdew, K. Burke, and M. Ernzerhof, Phys. Rev. Lett. **77**, 3865 (1996).

13. S. Nose, J. Chem. Phys. **81**, 511 (1984).

14. B. B. Karki, D. Bhattari, and L. Stixrude, Phys. Rev. **73**, 174208 (2006).

15. A. E. Galashev, Russ. J. Phys. Chem. A **96**, 2748 (2022).

16. A. Y. Galashev and Yu. P. Zaikov, J. Appl. Electrochem. **49**, 1027 (2019).

17. F. Philippi and T. Welton, Phys. Chem. Chem. Phys. **23**, 6993 (2021).
https://doi.org/10.1039/D1CP00216C

18. A. Y. Galashev, Appl. Sci. **13**, 1085 (2023).
https://doi.org/10.3390/app13021085

19. P. Calderoni, P. Sharpe, M. Hara, et al., Fusion Eng. Des. **83**, 1331 (2008).
https://doi.org/10.1016/j.fusengdes.2008.05.016

20. S. T. Lam, Q.-J. Li, J. Mailoa, et al., J. Mater. Chem. A **9**, 1784 (2021).
https://doi.org/10.1039/D0TA10576G

21. M. Pekar, ChemPhysChem. **16**, 884 (2015).
https://doi.org/10.1002/cphc.201402778

22. A. Y. Galashev, Nucl. Eng. Technol. (2023).
https://doi.org/10.1016/j.net.2022.12.029

Translated by Sh. Galyaltdinov